ORIGINAL ARTICLE

Exploring the Anti-Melanoma and Anti-Breast Cancer Potential of *Mitragyna speciosa* (Korth.) Havil. Leaf Constituents Using *In Silico* Approaches

Taslima Begum[1], Qamar Uddin Ahmed[1,*], ABM Helal Uddin[1], Mohd Hafiz Arzmi[2], Syed Adnan Ali Shah[3], Fezah Othman[4], Murni Nazira Sarian[5], Md. Abdur Rashid Mia[6], Muhammad Muzaffar Ali Khan Khattak[7]

[1]Drug Discovery and Synthetic Chemistry Research Group, Department of Pharmaceutical Chemistry, Kulliyyah of Pharmacy, International Islamic University Malaysia (IIUM), 25200 Kuantan, Pahang Darul Makmur, Malaysia; taslimabegum790@gmail.com (T.B.), quahmed@iium.edu.my (Q.U.A), abmhelal@iium.edu.my (A.B.M.H.U.)
[2]Department of Fundamental Dental and Medical Sciences, Kulliyyah of Dentistry, International Islamic University Malaysia, 25200 Kuantan, Pahang, Malaysia; hafizarzmi@iium.edu.my (M.H.A.)
[3]Faculty of Pharmacy, Atta-ur-Rahman Institute for Natural Products Discovery (AuRIns), Universiti Teknologi MARA, Cawangan Selangor Kampus Puncak Alam, 42300 Bandar Puncak Alam, Selangor, Malaysia; syedadnan@uitm.edu.my (S.A.S.)
[4]Department of Biomedical Sciences, Faculty of Medicine and Health Sciences, Universiti Putra Malaysia, Selangor, Malaysia; fezah@upm.edu.my (F.O.)
[5]Institute of Systems Biology (INBIOSIS), Universiti Kebangsaan Malaysia, 43600, Bangi, Selangor, Malaysia; murninazira@ukm.edu.my (M.N.S.)
[6]Cooperative Research, Extension, and Education Services (CREES), Northern Marianas College, P.O. Box 501250, Saipan MP 96950, USA.; mdabdur.mia@marianas.edu (M.R.M.)
[7]Food Security and Public Health Nutrition Research Group (Foster), Department of Nutrition Sciences, Kulliyyah of Allied Health Sciences, IIUM, 25200 Kuantan, Pahang Darul Makmur, Malaysia; muzaffar@iium.edu.my (M.M.A.K.K.)

Keywords:
Cancer, kratom, melanoma, breast cancer, *in silico*, binding affinity, drug-likeness.

Article history:
Received: 16 May 2026
Accepted: 23 June 2026
Published: 31 July 2026

ABSTRACT

Background: The incidence of melanoma and breast cancer globally are increasing at an alarming rate. However, many existing anticancer drugs are losing efficacy due to increasing drug resistance and are often accompanied by unavoidable side effects. This growing challenge underscores the urgent need for novel and selective anticancer therapies. Traditional medicinal plants, such as kratom (*Mitragyna speciosa* (Korth.) Havil.), offer promising avenues for drug discovery in this regard. **Methods:** This study explored the *in silico* anticancer potential of compounds identified in *M. speciosa* leaf extract using quadrupole time-of-flight liquid chromatography-mass spectrometry (Q-ToF-LCMS) analysis, alongside their physicochemical and pharmacokinetic parameters, to determine their suitability as lead candidates for anticancer drug development. A crude extract was prepared from kratom leaves using 100% methanol through ultrasound-assisted extraction yielding a 100% methanolic ultrasound-assisted extract with a recovery rate of 26.14%. The compounds were then screened *in silico* against two cancer-related proteins (PDB IDs: 3OG7 and 3ERT) to evaluate their potential against melanoma and breast cancer. **Results:** The identified phenolic, flavonoid, and alkaloidal compounds showed strong binding interactions with the melanoma target. Physicochemical and absorption, distribution, metabolism, excretion, and toxicity (ADMET) predictions revealed the potential of scopolin and 17-O-acetylajmaline as lead molecules for the development of new anticancer drugs to treat melanoma and breast cancer. **Conclusion:** The current study has identified promising lead compounds for the development of novel anticancer agents, providing a basis for future research on kratom-based anticancer drug discovery.

INTRODUCTION

Cancer is caused by abnormal cell division, affecting any organ in the body. It is considered one of the main causes of death across the globe (Bordoloi et al., 2018, Priatna et al., 2023). According to international statistics, twenty million new cancer cases and 9.7 million cancer-related fatalities were documented in 2022. Among these, skin melanoma ranked 17th in incidence, with 331,647 new cases and 58,645 deaths (Bray et al., 2024). Melanoma, often caused by ultraviolet exposure and carcinogenic BRAF mutations, is an aggressive form of skin cancer known for its rapid metastasis and progression (Banerjee et al., 2024, Umar et al., 2020). In contrast, breast cancer remains the most common malignancy among females globally. Approximately 70-80% of patients with early-stage, non-metastatic disease can be cured with current therapies. In contrast, advanced breast cancer characterised by distant organ metastases is regarded as incurable with currently accessible treatment options. At the molecular level, breast cancer is highly heterogeneous, with key characteristics including overactivation of human epidermal growth factor receptor 2 (HER2, encoded by ERBB2), hormone receptor signalling (oestrogen and

* *Corresponding author.*
E-mail address: quahmed@iium.edu.my

progesterone receptors), and/or mutations in BRCA genes (Harbeck et al., 2019).

Current cancer treatments, such as chemotherapy, impose a significant financial burden on patients (Smith et al., 2019) and are responsible for a range of deleterious effects due to their lack of selectivity towards cancer cells and the issue of multidrug resistance (Wang et al., 2019). Vemurafenib has been a preferred drug for treating melanoma; however, resistance to vemurafenib has already been reported (Banerjee et al., 2024). Similarly, toremifene is a drug of choice to treat breast cancer and has been found to be associated with cross-resistance to another anti-breast cancer drug, tamoxifen (Favoni & de Cupis, 1998).

Consequently, the development of new anticancer drugs has become a pressing need. Traditional medicinal plants, such as *Mitragyna speciosa* (Korth.) Havil. (locally known as kratom), offer promising anticancer compounds. This native plant of Southeast Asia is well-regarded by locals for its effectiveness in treating and preventing various diseases and disorders (Figure 1) (Begum et al., 2025a).

The anticancer potential of *M. speciosa* extracts and their constituents has been evaluated in various studies. For example, Goh et al. (2014) explored the properties of mitragynine and its silane-reduced analogue on erythroid leukaemia and colon carcinoma cell lines. Another study evaluated the cytotoxicity of hexane, dichloromethane (DCM), and methanol extracts of kratom against lung, colon and breast cancer cell lines (Rahman et al., 2022). Additionally, Zailan and coworkers (2019) assessed the cytotoxicity and cytokine inhibitory effects of the methanol extract on SW480 cells. Furthermore, Bayu et al. (2024) demonstrated that combining crude or alkaloid kratom extract with doxorubicin produced synergistic anticancer activity on the human lung cancer cell line (A549).

To date, only one *in silico* study has evaluated the anti-breast cancer activity of kratom alkaloids against estrogen receptor alpha (ERα) and P53 proteins, revealing their significant potential (Priatna et al., 2023). Kratom contains various compounds beyond alkaloids and evaluating different classes of these compounds against oncogenic protein targets can provide deeper insight. Therefore, an *in silico* study of kratom's identified compounds against mutant B-Raf Kinase protein in melanoma and against human estrogen receptor alpha in breast cancer would offer valuable information for both kratom and cancer treatment sectors. The aim of this study was to explore, through *in silico* approaches, the anticancer potential of compounds identified from *M. speciosa* leaf extracts. In addition, the study was also designed to characterise the physicochemical and pharmacokinetic characteristics of these compounds to explore their suitability as lead constituents for the development of novel anticancer agents.

Figure 1: A mature leaf of the kratom plant.

MATERIALS AND METHODS

Collection and Preparation of Plant Material

M. speciosa leaves were procured from Kedah, Malaysia. Species identification and authentication were performed at the KOP, IIUM, and a voucher specimen (voucher number PIIUM 0358) was deposited. The leaves were carefully cleaned and subsequently dried at 40 °C for 72 hours. Subsequently, the dried leaves were then pulverised using a Universal Cutting Mill (FRITSCH Pulverisette19, Germany) to obtain powdered kratom leaf material.

Preparation of Extract by Ultrasound-Assisted Extraction Method

Ultrasound-assisted extraction was performed to obtain a 100% methanolic ultrasound-assisted extract (100% US extract) of *M. speciosa* leaves. Briefly, 5 g of dried powdered leaf material was mixed with 50 mL of 100% methanol and placed in an ultrasonic extractor (UC-10, Jeio Tech Co., Ltd., Daejeon, Republic of Korea) for 30 minutes to obtain the ultrasonic extract (Figure 2). The resulting mixture was carefully filtered twice, and the resultant filtrate was concentrated under reduced pressure using a rotary evaporator. This process was repeated three times to ensure maximum yield. Lastly,

the percentage yield of the resultant extract was determined (Begum et al., 2025b).

Figure 2: Preparation of 100% US extract by ultrasound-assisted extraction method.

Identification of Compounds in the 100% US extract of *M. speciosa* leaf through Quadrupole Time-of-Flight Liquid Chromatography-Mass Spectrometry (Q-ToF-LCMS) analysis

The extract was analysed using an LC-MS/QTOF system (Agilent 1200 LC with an ESI source). Firstly, 1 mg of extract was dissolved in 250 µL of liquid chromatography grade methanol and subsequently vortexed and sonicated, and further mixed with 250 µL of distilled H_2O. The mixture was subjected to centrifugation for 15 minutes, and the supernatant was carefully transferred to a glass vial after filtration. Chromatographic separation was performed in a positive ionisation mode using two different mobile phases. The first phase consisted of 0.1% formic acid in water and the second phase consisted of 0.1% formic acid in acetonitrile. However, in negative ionisation mode, the first mobile phase consisted of 0.1% ammonium formate in water and the second consisted only of acetonitrile. The gradient program for both modes was: 0.0-18 min, 5-95% B; 18-23 min, 95% B; 23.01 min, 5% B. The total run time was 30 minutes, with a 2-minute re-equilibration before each injection. 2 µL was injected, and 0.25 mL/min was the flow rate of the mobile phase. The optimised conditions for the mass spectrometer were set as follows: gas flow 11 L/min, nebuliser pressure 35 psi and gas temperature 325 °C. Data files were processed using Agilent MHQA B.05.00 software (Agilent Technologies, SA, United States of America) (Begum et al., 2025c).

Molecular docking analysis

Q-ToF-LCMS analysis of the 100% ultrasonic methanolic extract of *M. speciosa* leaves identified several key phytoconstituents which were further investigated using *in silico* molecular docking. Chemical structures of the reference drugs (dabrafenib and toremifene) and the test compounds were retrieved from the PubChem database (https://pubchem.ncbi.nlm.nih.gov/). For docking studies, the human estrogen receptor alpha ligand-binding domain (PDB ID: 3ERT) (Shiau et al., 1998) and the BRaf kinase mutant (PDB ID: 3OG7) (Bollag et al., 2010) (Figure 3) were selected as target proteins and obtained from the Protein Data Bank (http://www.rcsb.org). Protein structures were prepared by removing water molecules and native ligands, followed by the addition of polar hydrogens. Redocking of the native ligand (vemurafenib) into 3OG7 was performed using grid points (X, Y, Z) set to 46, 16, and 36, respectively, with grid centre coordinates (X, Y, Z) at 2.643, -2.28, and -19.403, ensuring a root-mean-square deviation (RMSD) < 2. For 3ERT, redocking of the native ligand (OHT600) was carried out using grid points (X, Y, Z) set to 28, 28, and 28, with grid centre coordinates (X, Y, Z) at 30.01, -1.913, and 24.206, also ensuring RMSD < 2. AutoDock Tools 1.5.7 and AutoDock Vina were used for docking simulations (Trott et al., 2010), and Discovery Studio was used for visualisation and interaction analysis. Binding interactions were examined through both 2D and 3D representations to provide detailed insights (Umar et al., 2020).

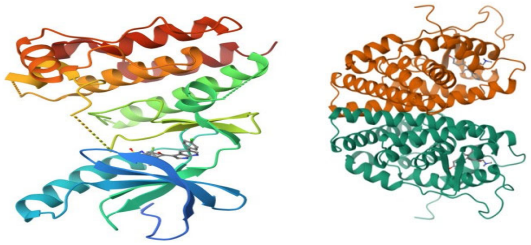

A **B**

Figure 3: 3D structures of two selected proteins: PDB ID 3OG7 (A) and PDB ID 3ERT (B) along with their respective native ligands retrieved from the Protein Data Bank.

Physicochemical and Pharmacokinetic Properties

The assessment of physicochemical and pharmacokinetic properties is a critical step in predicting drug disposition, maximising therapeutic outcomes, and safeguarding patient safety. Accordingly, the bioactive compounds identified from the 100% ultrasonic methanolic extract of *M. speciosa* leaves by Q-ToF-LCMS analysis were further assessed for their pharmacokinetic/physicochemical properties to investigate drug-likeness and other parameters including absorption, distribution,

metabolism, excretion, and toxicity (ADMET) profiles by utilising the SwissADME web server (accessed on 10 May 2026; http://www.swissadme.ch/index.php) and pkCSM web server (accessed on 10 May 2026; https://biosig.lab.uq.edu.au/pkcsm/prediction) (Ahmed et al., 2026).

RESULTS AND DISCUSSION

Yield of 100% US extract

Ultrasound-assisted extraction is widely recognised as an environmentally sustainable and highly efficient technique. By reducing or eliminating the use of organic solvents, it minimizes environmental impact while maintaining safety. Moreover, this method has been shown to markedly enhance the recovery of target bioactive compounds, making it an attractive and increasingly adopted approach in both research and industrial applications (Shen et al., 2023). Consequently, the 100% US extract of *M. speciosa* leaf was selected because of these advantages and was carefully prepared to support efficient extraction of bioactive compound. Therefore, the extract demonstrated a good yield, with a yield of 26.14%. This notable yield indicates the efficiency of the ultrasound-assisted extraction process in obtaining bioactive compounds from *M. speciosa* leaves.

Q-ToF-LCMS analysis

Q-ToF-LCMS afforded a robust basis for the identification of key phytoconstituents in the 100% ultrasonic methanolic extract of *M. speciosa* leaves. The analysis revealed a diverse range of metabolites, including phenolic compounds, flavonoids, and alkaloids (Table 1). Chromatograms obtained in both negative and positive ionisation modes offered a comprehensive overview of the extract's chemical profile (Figure 4). Representative chemical structures of selected identified compounds are presented in Figure 5.

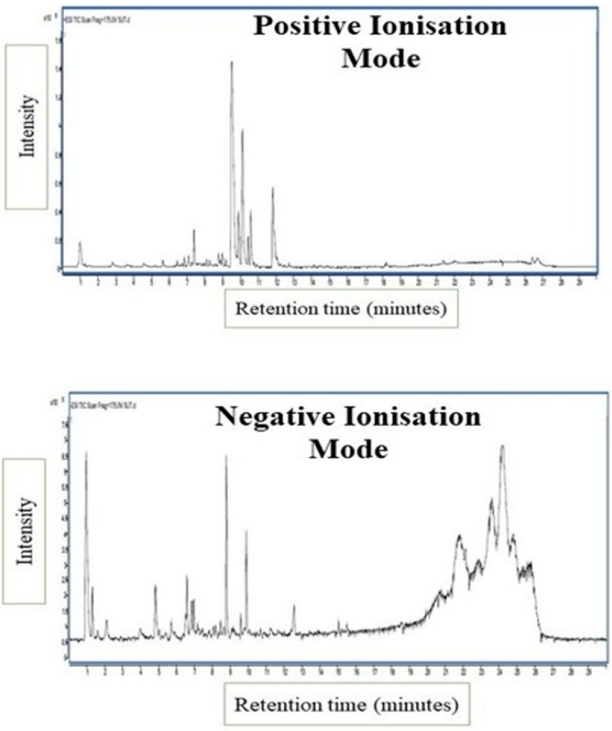

Figure 4: The Q-ToF-LCMS chromatograms of the 100% US leaf extract of *M. speciosa* in both negative and positive ionization modes.

Phenolic and flavonoid compounds are important plant secondary metabolites widely recognised for their significant biological properties (Chen et al., 2021). Flavonoids exert anticancer effects by halting cell division, invasion, and metastasis, as well as initiating apoptosis and cell-cycle arrest in cancer cells (Çetinkaya et al., 2022). Among the alkaloids, the anticancer properties of mitragynine have already been proven (Goh et al., 2014). Identified compounds such as scopolin can be converted into scopoletin in biological system, and reserpic acid and methyl respirate can be converted into reserpine. The anticancer properties of scopoletin and reserpine have been documented in several studies (Tian et al., 2021, Abdelfatah et al., 2025).

Table 1: The compounds identified in the 100% US extract of *M. speciosa* leaves through Q-ToF-LCMS analysis.

Putative Compounds	Molecular formula	Observed RT (min)	Score (%)	Observed *m/z*	Exact Mass (Da)	Mass Error (ppm)	Annotation Level
Scopolin	$C_{16}H_{18}O_9$	2.832	96.67	355.1032	354.09509	2.1	Level 2
Epifisetinidol-4alpha-ol	$C_{15}H_{14}O_6$	4.831	97.34	289.0715	290.07904	3.1	Level 2
Robinetinidol-(4alpha-8)-catechin-(6-4alpha)-robinetinidol	$C_{45}H_{38}O_{18}$	5.199	93.06	867.2115	866.20582	−2.5	Level 2

Formononetin 7-O-glucoside-6''-O-malonate	$C_{25}H_{24}O_{12}$	5.701	97.51	515.119	516.12678	0.1	Level 2
Robinetin 3-rutinoside	$C_{27}H_{30}O_{16}$	6.466	98.94	611.1612	610.15339	2.0	Level 2
5,6,7,3',4'-Pentahydroxy-8-methoxyflavone 7-apioside	$C_{21}H_{20}O_{12}$	6.743	99.11	465.1023	464.09548	−2.2	Level 2
8-Hydroxyluteolin 8-glucoside	$C_{21}H_{20}O_{12}$	6.856	94.97	463.0873	464.09448	5.3	Level 2
Luteolin 7-rhamnosyl(1-6)galactoside	$C_{27}H_{30}O_{15}$	7.079	97.5	595.1662	594.15848	0.4	Level 2
Reserpic acid	$C_{22}H_{28}N_2O_5$	7.895	98.57	401.2075	400.199823	0.6	Level 2
Methyl reserpate	$C_{23}H_{30}N_2O_5$	8.789	98.78	415.2234	414.215473	0.2	Level 2
17-O-Acetylajmaline	$C_{22}H_{28}N_2O_3$	9.187	99.09	369.2177	368.20999	−0.3	Level 2
Mitragynine	$C_{23}H_{30}N_2O_4$	9.893	96.14	399.2288	398.22056	1.0	Level 2

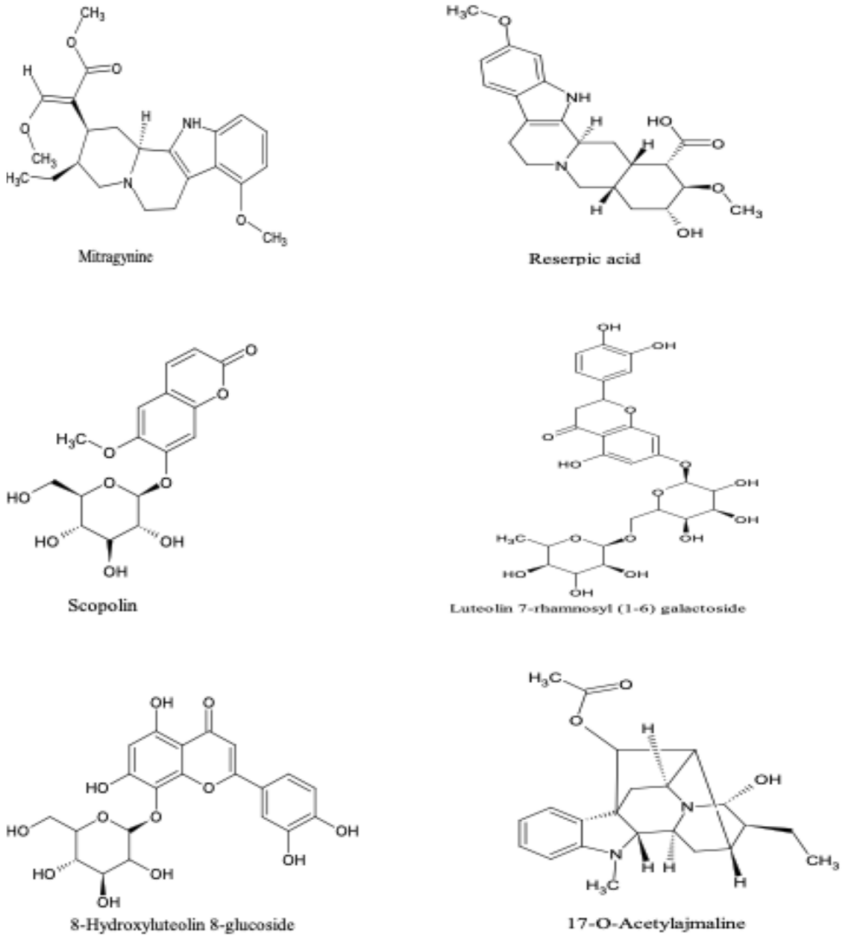

Figure 5: The chemical structures of some compounds identified by Q-ToF-LCMS analysis of the *M. speciosa* leaf's 100% US extract.

Table 2: Interaction profile of compounds from the 100% US extract of *M. speciosa* leaves with 3OG7 protein.

Compounds	Ligand binding energy (kcal/mol)	Binding Interactions	
		H bond interactions with bond distance (Å)	Other bond interactions with bond distance (Å)
Scopolin	-8.2	ASN 581: 2.89; CYS 532: 2.46; SER 465: 2.49	CYS 532: 4.70; TRP 531: 5.50; ALA 481: 4.21 & 5.18; LEU 514: 5.47 & 5.27; VAL 471: 4.42; PHE 583: 4.45 & 4.36
Epifisetinidol-4alpha-ol	-8.4	CYS 532: 2.85; ASP 594: 2.03	PHE 583: 3.91; CYS 532: 5.45; VAL 471: 5.30; LYS 483: 3.85
Robinetinidol-(4alpha-8)-catechin-(6-4alpha)-robinetinidol	-13.3	CYS 532: 2.33 & 3.16; LYS 483: 3.00; SER 465: 2.24; LYS 473: 2.01; TRP 531: 2.16; HIS 539: 2.51	HIS 539: 4.97; TRP 531: 5.91 & 3.65; ILE 463: 3.77
Formononetin 7-O-glucoside-6''-O-malonate	-9.2	SER 536: 2.00; CYS 532: 1.97; LYS 483: 2.61	LYS 483: 4.01; VAL 471: 3.58 & 3.92; LEU 514: 5.39 & 5.33; LEU 505: 3.94; ILE 527: 5.21; LEU 514: 5.39 & 5.33
Robinetin 3-rutinoside	-9.1	SER 536: 2.69 & 1.84; CYS 532: 2.49; SER 465: 1.82; ASN 580: 2.28; ASN 581: 1.93	VAL 471: 3.79 & 4.39; ALA 481: 5.47
5,6,7,3',4'-Pentahydroxy-8-methoxyflavone 7-apioside	-8.9	ILE 527: 2.28; CYS 532: 2.10; SER 536: 2.21; ASN 580: 2.46 & 2.85	LYS 483: 4.81; ALA 481: 4.68 & 4.76; VAL 471: 4.62, 4.79 & 5.47; ILE 463: 5.32; TRP 531: 5.59 & 5.81; PHE 583: 4.52 & 4.69
8-Hydroxyluteolin 8-glucoside	-10.4	ASN 580: 3.22; ASN 581: 3.36; GLN 530: 3.30; ALA 481: 3.12; THR 529: 3.21; ILE 527: 2.99	ASP 594: 4.96; VAL 471: 5.49, 4.36 & 5.15; TRP 531: 5.36; PHE 583: 4.48; CYS 532: 5.26; ALA 481: 4.59
Luteolin 7-rhamnosyl(1-6)galactoside	-10.5	CYS 532: 2.62 & 3.03; ASP 594: 2.52; LYS 483: 2.76; ASN 580: 2.22; LYS 578: 2.76	-
Reserpic acid	-8.6	ASN 581: 2.32; ASN 580: 2.74	ALA 481: 5.14; LYS 483: 3.95; ILE 527: 4.72; VAL 471: 3.58 & 4.42
Methyl reserpate	-9.1	SER 536: 2.74 & 2.69	VAL 471: 3.91 & 4.43; ALA 481: 5.06 & 3.72; PHE 583: 4.59 & 4.43; LEU 514: 4.50; CYS 532: 3.84
17-O-Acetylajmaline	-8.1	SER 536: 2.88	ALA 481: 5.16; VAL 471: 3.78
Mitragynine	-8.6	-	PHE 583: 3.93; 5.21 & 4.85

Native Ligand (Vemurafenib)	-11.1	GLN 530: 2.24; GLY 596: 2.21; PHE 595: 2.68	ILE 463: 4.66; TRP 531: 5.93; CYS 532: 5.00; LEU 505: 4.06; LYS 483: 4.10; PHE 583: 4.75; LEU 514: 4.83; ALA 481: 3.79; PHE 595: 4.59
Standard drug (Dabrafenib)	-9.0	ASP 594: 2.60; ASN 590: 1.83	PHE 468: 5.09; LYS 578: 4.27; SER 465: 3.27; ASN 580: 3.29; ASP 594: 3.13; ASN 581: 3.57; VAL 471: 4.70 & 5.07; TRP 531: 5.02; PHE 583: 4.50 & 3.53

Molecular Docking Analysis

To investigate the potential anticancer activity of the Q-ToF-LCMS identified compounds, molecular docking was performed against two therapeutically relevant targets associated with melanoma and breast cancer. The first target, BRAF kinase (PDB ID: 3OG7), is a serine/threonine protein kinase, which functions as a key regulator of growth signal transduction. It plays a central role in the mitogen-activated protein kinase (MAPK)/ERK signalling pathway signalling pathway, influencing cellular processes such as cell division, differentiation, and secretion. The oncogenic BRAF V600E mutation results in constitutive activation of downstream signalling, promoting uncontrolled cell proliferation, increased cancer aggressiveness and reduced chemotherapy efficacy, as they diminish tumour responsiveness to anticancer agents. Consequently, direct inhibition of the mutated B-Raf kinase has emerged as an effective therapeutic strategy and a significant advance in oncology. The crystal structure 3OG7 contains the clinically approved inhibitor vemurafenib bound within the ATP-binding catalytic pocket, a well-characterized and highly druggable site that has been successfully utilized for the development of targeted melanoma therapies (Hassan et al., 2022; Tsai et al., 2008; Davies et al., 2002; Bollag et al., 2010; Cope et al., 2019). Therefore, this structure was selected as a biologically relevant model for evaluating the binding affinities of the identified compounds toward a validated melanoma target.

The docking analysis of 3OG7 protein revealed that the native ligand (vemurafenib) showed an RMSD of 0.594, with an affinity binding energy of -11.1 kcal/mol. Moreover, standard (dabrafenib) exhibited a binding score of -9.0 kcal/mol. Among the identified compounds, robinetinidol-(4alpha-8)-catechin-(6-4alpha)-robinetinidol demonstrated the highest binding affinity (-13.3 kcal/mol), while 17-O-acetylajmaline exhibited the lowest binding affinity (-8.1 kcal/mol) (Table 2). The binding interactions of the native ligand, dabrafenib, formononetin 7-O-glucoside-6''-O-malonate, robinetinidol-(4alpha-8)-catechin-(6-4alpha)-robinetinidol, scopolin, and 17-O-acetylajmaline with the 3OG7 are illustrated in Figure 6a. Moreover, the binding interaction of the other compounds are provided in Figure 6b.

The molecular docking results revealed that the compounds, including the controls, interacted with the protein via various types of bonds. For the native ligand, three amino acids were responsible for conventional hydrogen bonds: GLN 530, GLY 596, and PHE 595, along with hydrophobic interactions with ILE 463, TRP 531, CYS 532, LEU 505, LYS 483, PHE 583, LEU 514, ALA 481, PHE 595.

In the case of robinetinidol-(4alpha-8)-catechin-(6-4alpha)-robinetinidol, conventional hydrogen bonds were observed with CYS 532, LYS 483, SER 465, LYS 473, TRP 531, and HIS 539, and hydrophobic interactions with HIS 539, TRP 531, and ILE 463. Moreover, luteolin 7-rhamnosyl (1-6) galactoside formed conventional hydrogen bonds with CYS 532, ASP 594, LYS 483, ASN 580, and LYS 578.
Conversely, 17-o-acetylajmaline, which had the lowest binding interaction, was involved with SER 536 through hydrogen bonding and with ALA 481 and VAL 471 through hydrophobic interactions. Additionally, in the case of scopolin, ASN 581, CYS 532, and SER 465 were responsible for conventional hydrogen bonds and CYS 532, TRP 531, ALA 481, LEU 514, VAL 471, and PHE 583 were responsible for other interactions.

The standard drug, dabrafenib interacted with ASP 594 and ASN 590 via hydrogen bonding and with PHE 468, LYS 578, SER 465, ASN 580, ASP 594, ASN 581, VAL 471, TRP 531, and PHE 583 for other hydrophobic interactions. Thus, the compounds and the standard drug interacted with the catalytic site of the PDB ID: 3OG7 with amino acids similar to those of the native ligand. CYS 532, LYS 483, TRP 531, and ALA 481 were the amino acids most commonly present in their interactions. Thus, the compounds identified from the 100% ultrasonic methanolic extract demonstrated strong binding affinities, along with the interaction at the catalytic site of the protein, suggesting their potential to inhibit oncogenic B-Raf kinase activity.

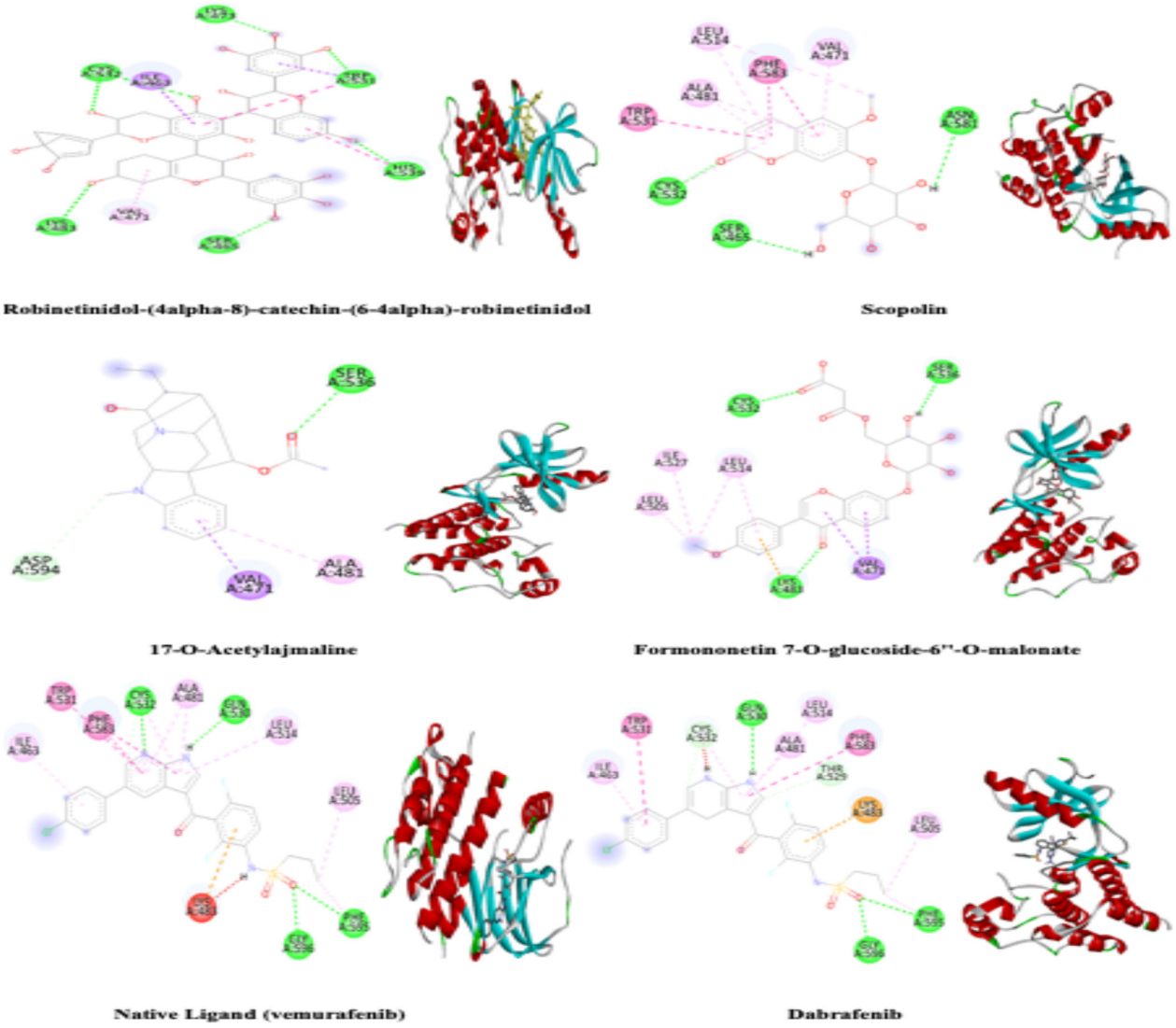

Figure 6a: Binding interactions of robinetinidol-(4alpha-8)-catechin-(6-4alpha)-robinetinidol, scopolin, 17-O-acetylajmaline, and formononetin 7-O-glucoside-6''-O-malonate along with the native ligand and dabrafenib with the 3OG7 protein.

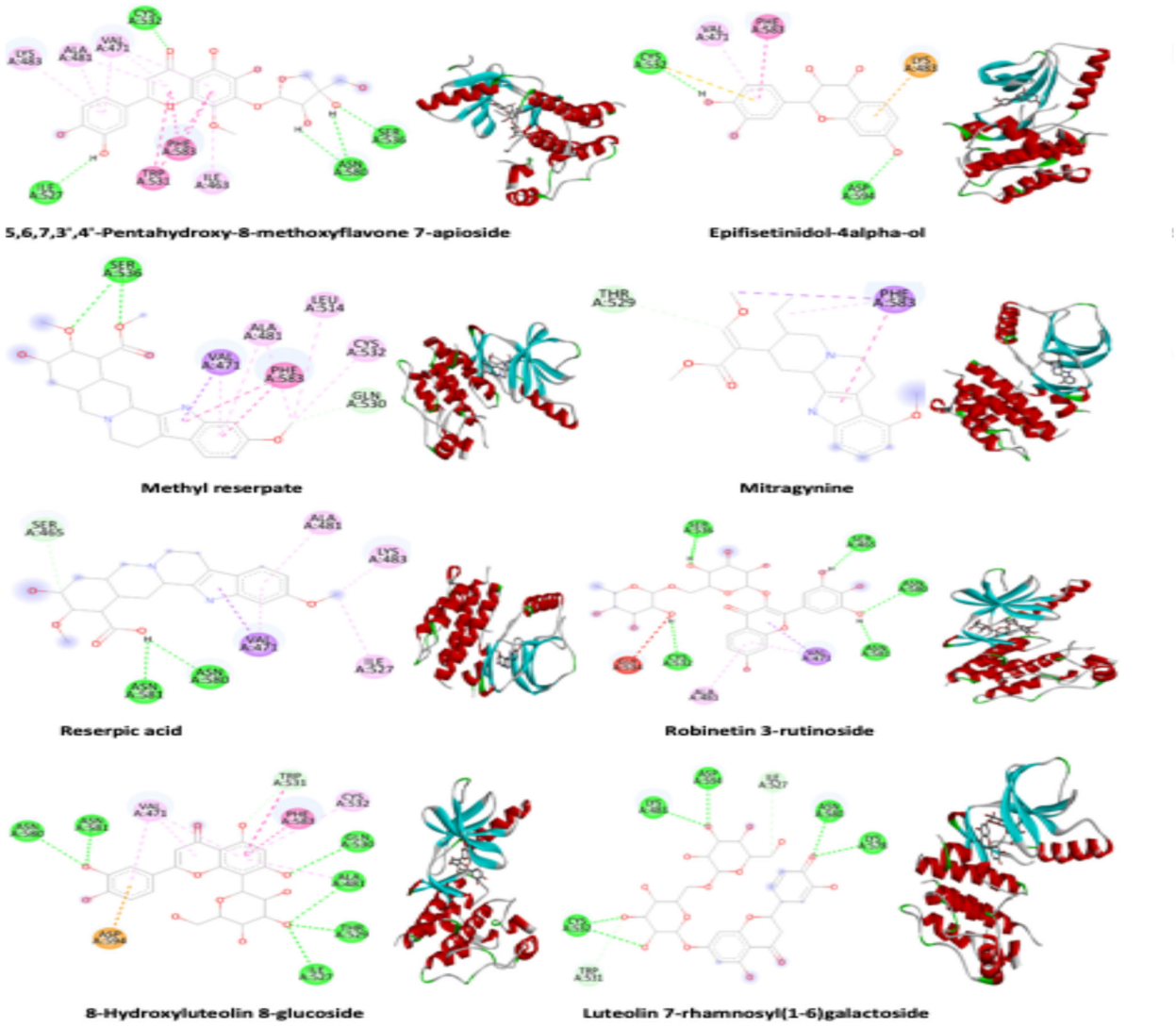

Figure 6b: Binding interactions of other compounds with the 3OG7 protein.

The second protein target, estrogen receptor alpha (ERα) (PDB ID: 3ERT), is a ligand-activated nuclear receptor that functions as a DNA-binding transcription factor that regulates gene expression and diverse cellular processes. ERα is expressed in approximately 70% of all human breast cancers and clinical evidence strongly supports a role of ERα in breast cancer. The crystal structure 3ERT contains 4-hydroxytamoxifen bound to the receptor's canonical ligand-binding (orthosteric) pocket, a therapeutically validated site targeted by several endocrine therapies used in breast cancer treatment (Shiau et al., 1998; Shanle & Xu, 2010). Owing to its established role in breast cancer progression and proven druggability, ERα was selected as an appropriate target for virtual screening and molecular interaction studies.

Likewise, for the 3ERT protein, the native ligand (OHT600) and toremifene (standard drug) exhibited binding energies of -9.9 and -8.7 kcal/mol, respectively. Among the identified compounds, robinetinidol-(4alpha-8)-catechin-(6-4alpha)-robinetinidol exhibited the strongest binding energy (-11.3 kcal/mol), followed by formononetin 7-O-glucoside-6''-O-malonate (-8.7 kcal/mol), luteolin 7-rhamnosyl (1-6)galactoside (-8.6 kcal/mol) and 17-O-acetylajmaline (-8.4 kcal/mol). Among the compounds, mitragynine showed the lowest binding energy (-7.0 kcal/mol). Table 3 contains the binding interactions of all the identified compounds against the 3ERT protein. The binding interactions of robinetinidol-(4alpha-8)-catechin-(6-4alpha)-robinetinidol, scopolin, 17-O-acetylajmaline, and formononetin 7-O-glucoside-6''-O-malonate along with the native ligand and dabrafenib with the 3ERT protein are shown in Figure 7a. Moreover, the binding interactions of the rest of the compounds are presented in Figure 7b.

Table 3: Interaction profile of compounds from the 100% US extract of *M. speciosa* leaves with 3ERT protein

Compounds	Ligand binding energy (kcal/mol)	Binding Interactions	
		H bond interactions with bond distance (Å)	Other bond interactions with bond distance (Å)
Scopolin	-7.5	-	LEU 346: 5.42; ALA 350: 4.71 & 4.77; MET 343: 5.33, 4.71 & 5.04; LEU 525: 3.91 & 4.69; MET 421: 4.69
Epifisetinidol-4alpha-ol	-8.0	ARG 394: 2.00; GLU 353: 2.16; THR 347: 2.30	MET 343: 4.92; LEU 346: 4.65; LEU 525: 3.87; ALA 350: 5.48 & 4.12; LEU 391: 4.97; LEU 387: 4.32
Robinetinidol-(4alpha-8)-catechin-(6-4alpha)-robinetinidol	-11.3	VAL 534: 3.24; VAL 533: 3.22; LEU 536: 2.45; CYS 530: 3.44; MET 528: 3.35	MET 528: 3.87; CYS 530: 5.08; MET 522: 5.29; TYR 526: 5.01; LEU 536: 5.46; ALA 350: 5.29; LEU 525: 4.40
Formononetin 7-O-glucoside-6''-O-malonate	-8.7	HIS 524: 2.16; GLY 420: 2.93; CYS 530: 2.06	CYS 530: 5.38; VAL 533: 4.86; LYS 529: 3.88; ALA 350: 4.00; LEU 346: 5.02; LEU 525: 3.64; MET 343: 5.05 & 5.02
Robinetin 3-rutinoside	-8.0	CYS 530: 2.19; ASP 351: 2.43; MET 522: 2.68	MET 522: 3.98; LEU 525: 4.49 & 4.49; LYS 529: 5.44
5,6,7,3',4'-Pentahydroxy-8-methoxyflavone 7-apioside	-7.9	MET 522: 2.14	LEU 536: 5.28; MET 343: 4.96; ALA 350: 3.97 & 5.01; LEU 525: 5.34 & 4.65
8-Hydroxyluteolin 8-glucoside	-8.2	MET 528: 2.91; CYS 530: 1.90; MET 343: 3.62	MET 343: 5.08; LEU 525: 3.92; ALA 350: 4.03 & 4.87; ASP 351: 3.46 & 3.63
Luteolin 7-rhamnosyl (1-6)galactoside	-8.6	LEU 525: 3.21; LEU 536: 1.96 & 2.69; CYS 530: 2.22	MET 522: 5.33
Reserpic acid	-7.9	ASP 351: 2.53	MET 522: 3.98 & 4.04
Methyl reserpate	-7.5	-	ALA 350: 5.17, 4.09 & 3.85; LEU 525: 3.91 & 3.86; LEU 346: 4.75 & 4.75; MET 343: 5.91 & 5.08
17-O-Acetylajmaline	-8.4	-	MET 522: 4.64; TYR 526: 4.94; LEU 536: 4.07
Mitragynine	-7.0	-	LEU 536: 4.88; LEU 525: 5.46 & 5.25; ALA 350: 4.71 & 4.07; LEU 354: 3.89; TRP 383: 4.33
Native Ligand: OHT600	-9.9	GLU 353: 2.50	LEU 346: 4.98 & 4.94; MET 421: 4.77 & 5.24; LEU 525: 4.88 & 4.78; ALA 350: 4.12; LEU 387: 5.01
Standard drug: Toremifene	-8.7	-	ALA 350: 4.02 & 4.41; LEU 387: 5.10; LEU 346: 4.71; LEU 525: 4.68 & 4.90; LEU 391: 4.61; MET 388: 3.57; LEU 428: 4.48; MET 421: 5.13

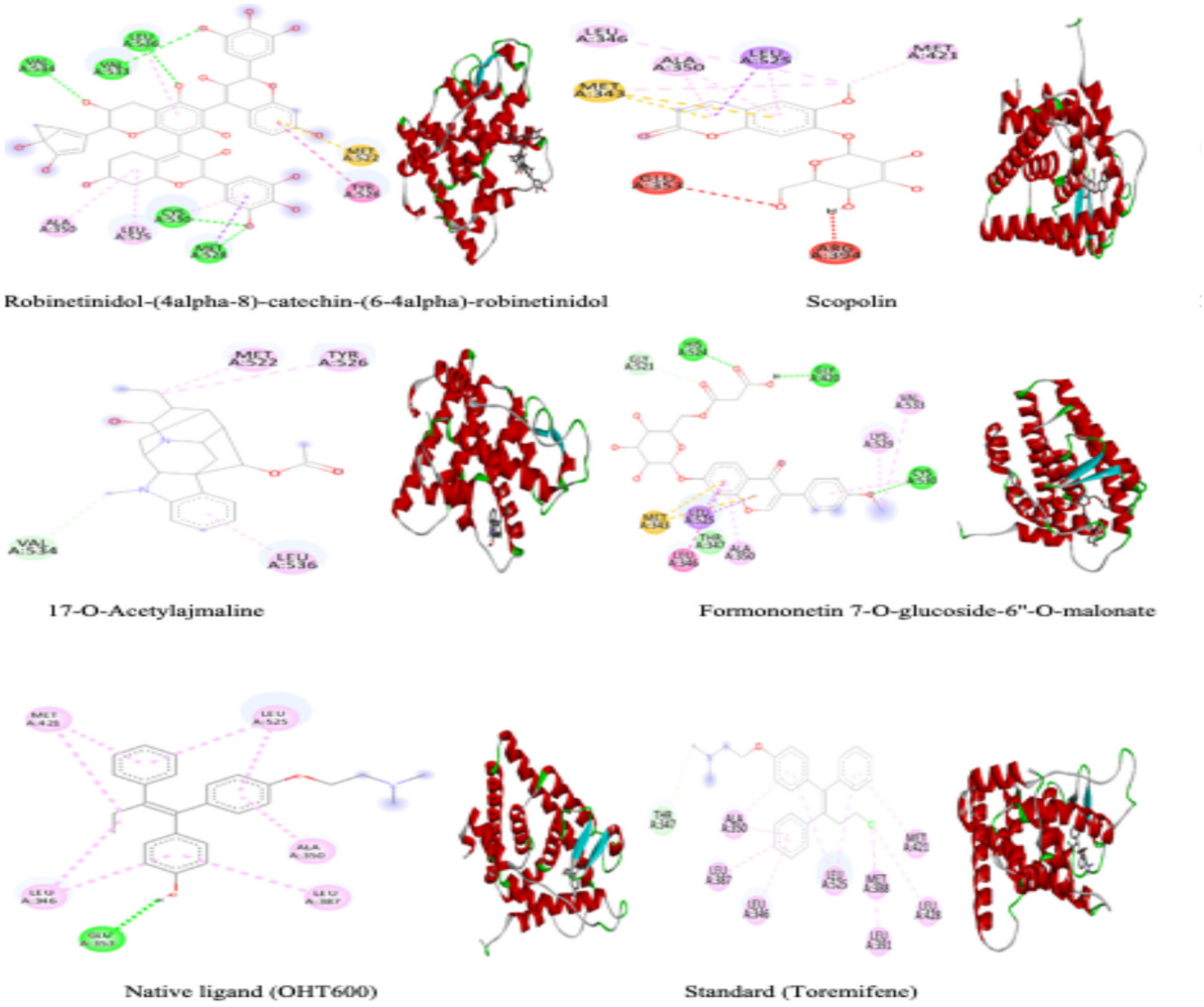

Figure 7a: Binding interactions of robinetinidol-(4alpha-8)-catechin-(6-4alpha)-robinetinidol, scopolin, 17-o-acetylajmaline, and formononetin 7-O-glucoside-6''-O-malonate along with the native ligand and toremifene with 3ERT protein.

The native ligand (OHT600) formed a hydrogen bond with GLU 353 of 3ERT, while additional interactions were observed with LEU 346, MET 421, LEU 525, ALA 350, and LEU 387. Robinetinidol-(4alpha-8)-catechin-(6-4alpha)-robinetinidol showed hydrogen bonds with VAL 534, VAL 533, LEU 536, CYS 530, and MET 528. Moreover, other binding interactions were observed with MET 528, CYS 530, MET 522, TYR 526, LEU 536, ALA 350, and LEU 525. Formononetin 7-O-glucoside-6''-O-malonate showed hydrogen bonds with HIS 524, GLY 420, and CYS 530, as well as other interactions with CYS 530, VAL 533, LYS 529, ALA 350, LEU 346, LEU 525, and MET 343. Luteolin 7-rhamnosyl (1-6) galactoside formed hydrogen bonds with LEU 525, LEU 536, and CYS 530. Scopolin exhibited hydrophobic interactions with LEU 346, ALA 350, MET 343, LEU 525, and MET 421. Moreover, LEU 536, LEU 525, ALA 350, LEU 354, and TRP 383 were involved in the non-hydrogen bond interactions, in the case of mitragynine. Furthermore, the standard drug, toremifene showed diverse interactions with amino acids, including ALA 350, LEU 387, LEU 346, LEU 525, LEU 391, MET 388, LEU 428, and MET 421. Overall, the tested compounds demonstrated comparable amino acid involvement to that observed with both the native ligand and the standard drug, and ALA 350 and LEU 525 were found to be the common amino acids. The standard drug, toremifene, a selective estrogen receptor modulator, exerts mixed estrogenic and anti-estrogenic effects. In breast tissue, it competes with estrogen for receptor binding sites, thereby producing antiestrogenic and antitumor effects (Martinkovich et al., 2014). Since the identified compounds showed similar interactions as the toremifene, they might also possess a great potential as anti-breast cancer agents. Estrogen receptors (ERs) are nuclear

receptors located in the cytoplasm that function as DNA-binding transcription factors, regulating gene expression and diverse cellular processes. Two isoforms of the human estrogen receptor exist, ERα and ERβ, both of which have been implicated in breast cancer pathogenesis. Structurally, ERs comprise three major domains: the DNA-binding domain, the ligand-binding domain, and the transactivation domain (McGee et al., 2008).

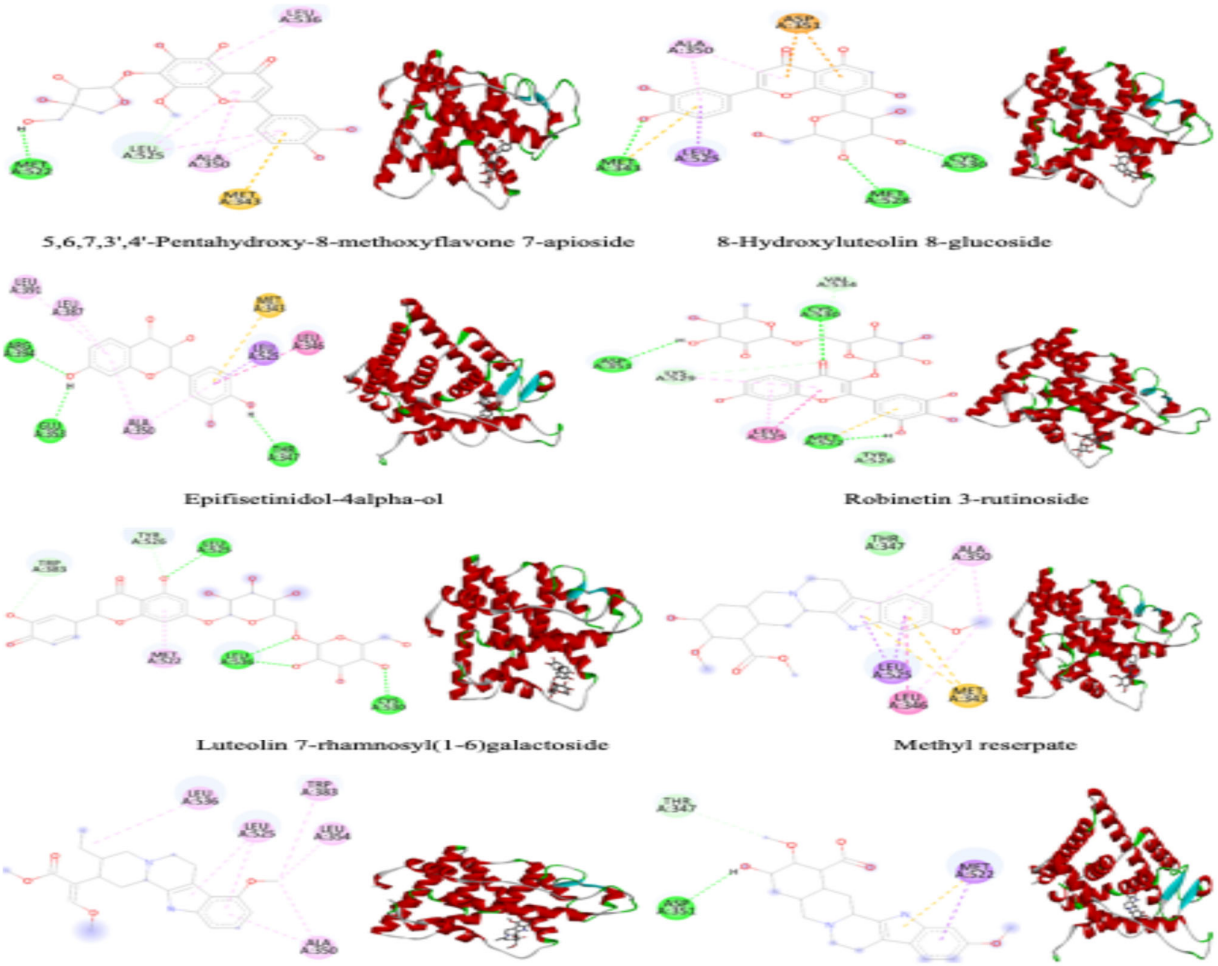

Figure 7b: Binding interactions of other compounds with 3ERT protein.

Table 4: The physicochemical and ADMET parameters of the compounds from the methanol extract of *M. speciosa* leaves.

Compound	Properties										
	Physicochemical						ADMET				
	MW	Log P	NHA	NHD	NLV	DL	IA	CLR	HET	AM	ROAT
5,6,7,3',4'-Pentahydroxy-8-methoxyflavone 7-apioside	464.38	-2.32	12	7	2	No	41.382	0.439	No	No	2.61
Epifisetinidol-4alpha-ol	290.27	-0.02	6	5	0	Yes	65.555	0.003	No	Yes	2.45
17-O-Acetylajmaline	368.47	3.00	4	1	0	Yes	97.092	0.896	No	No	2.886
8-Hydroxyluteolin 8-glucoside	464.38	-2.59	12	8	2	No	33.475	0.384	No	No	2.562
Luteolin 7-rhamnosyl (1-6)galactoside	594.52	-3.43	15	9	3	No	27.777	0.251	No	Yes	2.734

Mitragynine	398.50	2.02	5	1	0	Yes	92.967	0.859	Yes	No	3.157
Formononetin 7-O-glucoside-6''-O-malonate	516.45	-1.06	12	4	2	No	40.995	0.333	No	No	2.617
Reserpic acid	400.47	1.08	6	3	0	Yes	61.972	0.433	Yes	No	2.1
Robinetin 3-rutinoside	610.52	-3.89	16	10	3	No	20.596	-0.377	No	No	2.49
Methyl reserpate	414.49	1.30	6	2	0	Yes	93.519	48.119	Yes	No	2.93
Scopolin	354.31	-1.23	9	4	0	Yes	48.119	0.716	No	No	2.391
Robinetinidol-(4alpha-8)-catechin-(6-4alpha)-robinetinidol	866.77	-1.11	18	15	3	No	33.083	33.083	No	No	2.482

Note: MW: molecular weight, gram/mole; Log P: predicted octanol/water partition coefficient; NHA: number of hydrogen bond acceptors; NHD: number of hydrogen bond donor; D: drug-likeness; NVL: number of Lipinski's rule violations; IA: intestinal absorption, %; CLR: clearance; (log ml/min/kg); HET: hepatotoxicity; AM: AMES toxicity; ROAT: rat acute oral toxicity, mol/kg.

Physicochemical and Pharmacokinetic Profiles of Compounds from *M. speciosa* leaf Methanol Extract

The drug discovery and development is a challenging, time-consuming, intricate, and costly endeavour, often associated with uncertainty regarding clinical success. To streamline these processes, predicting the ADMET (Absorption, Distribution, Metabolism, Excretion, and Toxicity) properties of a compound before it enters clinical trials allows potential issues to be indentified early in the development process (De Carlo et al., 2024). In this context, predicting the physicochemical and pharmacokinetic parameters of the identified compounds from the 100% US extract, which also showcased potent inhibition of the oncogenic B-Raf Kinase protein, could be highly beneficial. This approach may aid in the development of new selective anticancer drugs against melanoma based on these compounds. Thus, the physicochemical and pharmacokinetic parameters of the compounds from *M. speciosa* leaf's methanol extract were thoroughly evaluated (Table 4).

The physicochemical profiling of the 12 identified compounds revealed that 6 exhibited drug-like properties, with minimal violations of the Lipinski Rule of Five (Salihu et al., 2024). Subsequent ADMET evaluation indicated that among these, scopolin and 17-O-acetylajmaline demonstrated promising potential as lead candidates for the development of selective anticancer agents. These compounds showed favourable intestinal absorption rates of 48.119% and 97.092%, respectively, and were free from both hepatotoxicity and AMES toxicities. To improve the intestinal absorption or mitigate toxicity risks, several strategies in drug design have proven effective, including particle size reduction, surface area enhancement, and prodrug formation (Alagga et al., 2025, Jornada et al., 2015). Conversely, mitragynine and methyl reserpate demonstrated high intestinal absorption rates of 92.967% and 93.519%, respectively, but were associated with hepatic toxicity. Moreover, ent-fisetinidol-4beta-ol and reserpic acid, showed moderate intestinal absorption yet also presented hepatic toxicity concerns.

Importantly, robinetinidol-(4alpha-8)-catechin-(6-4alpha)-robinetinidol, luteolin 7-rhamnosyl (1-6)galactoside, 8-hydroxyluteolin 8-glucoside, formononetin 7-O-glucoside-6''-O-malonate and robinetin 3-rutinoside showed strong binding affinities in molecular docking analyses. Despite their promising interactions with target proteins, these compounds lacked drug-likeness due to their high molecular weights and high polarity, which significantly hindered their absorption across biological membranes. To enhance their pharmacokinetic profiles, the incorporation of hydrophobic moieties has been suggested as a viable strategy to increase lipophilicity and facilitate systemic absorption, thereby increasing their suitability for drug development (Begum et al., 2025b).

Comprehensive evaluation through Q-TOF LC-MS profiling, molecular docking, and physicochemical and pharmacokinetic assessments revealed that the 100% US extract of *M. speciosa* leaf contains a diverse array of phenolic, flavonoid, and alkaloidal compounds. Among these, only scopolin and 17-O-acetylajmaline demonstrated favourable drug-like properties and ADMET profiles, positioning them as promising lead candidates for the development of selective anticancer therapeutics.

CONCLUSION

The biological activities of plant extracts and their individual compounds can differ markedly due to the complex nature of phytochemical interactions. Extracts typically contain complex mixtures of compounds that

may synergise or antagonise each other's effects. Consequently, the therapeutic potential of certain bioactive constituents may be masked or diminished when assessed within the whole extract. Therefore, the identification and isolation of potent compounds from crude extracts represent a strategic approach in the discovery and rational design of novel drug candidates. Currently, many available anticancer drugs lack selectivity and are associated with significant adverse effects. This limitation underscores the urgent need for the development of new, selective anticancer drugs derived from natural sources. Based on the findings of the current study, scopolin and 17-O-acetylajmaline have emerged as promising lead compounds for the development of anticancer drugs against melanoma and breast cancer. The findings of this study are hypothesis-generating and suggest that the identified compounds may represent promising candidates for further investigations rather than confirmed anticancer leads. Future studies should prioritise experimental validation through biochemical target-binding assays, *in vitro* cytotoxicity testing against relevant melanoma and breast cancer cell lines, and preliminary ADME evaluations to verify the computational predictions and establish their therapeutic potential.

ACKNOWLEDGEMENT

This study was partially supported by CRIGS UKM-IIUM-UiTM-UPM Research Collaboration Grant 2024 (C-RIGS24-017-0023), Research Management Centre, International Islamic University Malaysia (IIUM), Malaysia. All authors are also thankful to Regal Malay Capital Berhad, Malaysia (SPP22-137-0137).

AUTHOR CONTRIBUTIONS

Conceptualization, Q.U.A.; M.M.A.K.K.; T.B.; methodology, T.B.; Q.U.A.; resources, Q.U.A.; M.H.A.; data curation, T.B.; M.S.R.; S.A.A.S.; F.O.; writing-original draft preparation, T.B.; writing-review and editing, Q.U.A.; M.M.A.K.K.; M.N.S.; visualization, Q.U.A.; A.B.M.H.U.; M.N.S.; M.R.M.; supervision, Q.U.A. All authors have read and agreed to the published version of the manuscript.

CONFLICT OF INTEREST

The authors declare that they have no conflicts of interest.

DATA AVAILABILITY

Data will be made available on reasonable request.

ETHICAL APPROVAL

Not applicable.

REFERENCES

Abdelfatah, S. A., & Efferth, T. (2015). Cytotoxicity of the indole alkaloid reserpine from Rauwolfia serpentina against drug-resistant tumor cells. *Phytomedicine, 22*(2), 308-318. https://doi.org/10.1016/j.phymed.2015.01.002

Ahmed, Q. U., Ab Rahim, M. A. H., Arzmi, M. H., Uddin, A. H., Ali Shah, S. A., Rofiee, M. S., Parveen, H., Mukhtar, S., Faridi, U., Rosedi, N. H. M., Sarian, M. N. & Begum, T. (2026). Antimicrobial and antioxidant activities of *Tetracera macrophylla* Hook. f. & Thomson leaf extracts: insights from Q-ToF-LCMS, pharmacokinetics and molecular docking approach. *Natural Product Research*, 1-15. https://doi.org/10.1080/14786419.2026.2654646.

Alagga, A. A., Pellegrini, M. V., & Gupta, V. (2024). Drug absorption. In StatPearls [Internet]. StatPearls Publishing. Available from: https://www.ncbi.nlm.nih.gov/books/NBK557405/

Banerjee, S., bharkatiya, M., Rao, S. P., & Baghel, I. (2024). Exploration of anti-melanoma potential of phytochemicals from *Nyctanthes arbortristis* through computational studies. *International Journal of Applied Pharmaceutics, 16*(2), 166-173. https://dx.doi.org/10.22159/ijap.2024v16i2.49834

Bayu, A., Rahmawati, S. I., Karim, F., Panggabean, J. A., Nuswantari, D. P., Indriani, D. W., Ahmadi, P., Witular, R., Dharmayanti, N. L. P. I., & Putra, M. Y. (2024). An *in vitro* examination of whether kratom extracts enhance the cytotoxicity of low-dose doxorubicin against A549 human lung cancer cells. *Molecules, 29*(6), 1404. https://doi.org/10.3390/molecules29061404

Begum, T., Arzmi, M. H, Khatib, A., Uddin, A. H., Aisyah Abdullah, M., Rullah, K., Mat So'ad, S. Z., Haspi, N. F. Z., Sarian, M. Z., Parveen, H., Mukhtar, S., & Ahmed, Q. U. (2025a). A Review on *Mitragyna speciosa* (Rubiaceae) as a Prominent Medicinal Plant Based on Ethnobotany, Phytochemistry and Pharmacological Activities. *Natural Product Research, 39*(6), 1636-1652. https://doi.org/10.1080/14786419.2024.2371564

Begum, T., Arzmi, M. H., Uddin, A. H, Rofiee, M. S., Shah, S. A. A., Parveen, H., Mukhtar, S., Ahmed, Q. U. (2025b). Unveiling comparative bioactivities of Kratom leaf extracts obtained via maceration and ultrasonic techniques: Antioxidant, antimicrobial, and antibiofilm effects with molecular docking of Q-ToF-LCMS identified compounds and ADMET prediction. *Journal of King Saud University–Science,*

37(10). https://doi.org/10.25259/JKSUS_1185_2025

Begum, T., Ahmed, Q. U., Arzmi, M. H., Uddin, A. H., Khatib, A., Mohamad, S. N. A. S., Nasarudin, S. N. I. S., Abbas, S.A., Abd Aziz, Z. H. (2025c). Phytochemical screening and evaluation of *in vitro* antioxidant, antibacterial and antibiofilm activities of *Mitragyna speciosa* leaf extract. *Malaysian Journal of Chemistry, 27*(5), 80-94. https://doi.org/10.55373/mjchem.v27i5.80

Bollag, G., Hirth, P., Tsai, J., Zhang, J., Ibrahim, P. N., Cho, H., Spevak, W., et al. (2010). Clinical efficacy of a RAF inhibitor needs broad target blockade in BRAF-mutant melanoma. *Nature, 467*(7315), 596-599. https://doi.org/10.1038/nature09454

Bordoloi, D., Sailo, B. L., Manteghi, N., Padmavathi, G., & Kunnumakkara, A. B. (2018). Introduction and basic concepts of cancer. In Cancer cell chemoresistance and chemosensitization (pp. 1-13). https://doi.org/10.1142/9789813208575_0001

Bray, F., Laversanne, M., Sung, H., Ferlay, J., Siegel, R. L., Soerjomataram, I., & Jemal, A. (2024). Global cancer statistics 2022: GLOBOCAN estimates of incidence and mortality worldwide for 36 cancers in 185 countries. CA: A Cancer Journal for Clinicians, 74(3), 229-263. https://doi.org/10.3322/caac.21834

Çetinkaya, S., Akça, K. T., & Süntar, I. (2022). Flavonoids and anticancer activity: Structure–activity relationship. *Studies in Natural Products Chemistry, 74*, 81-115. https://doi.org/10.1016/B978-0-323-91099-6.00017-7

Chen, Q., Wang, X., Yuan, X., Shi, J., Zhang, C., Yan, N., & Jing, C. (2021). Comparison of phenolic and flavonoid compound profiles and antioxidant and α-glucosidase inhibition properties of cultivated soybean (Glycine max) and wild soybean (*Glycine soja*). *Plants, 10*(4), 813. https://doi.org/10.3390/plants10040813

Cope, N., Novak, B., Candelora, C., Wong, K., Cavallo, M., Gunderwala, A., Liu., Z., Li., Y., & Wang, Z. (2019). Biochemical Characterization of Full-Length Oncogenic BRAFV600E together with Molecular Dynamics Simulations Provide Insight into the Activation and Inhibition Mechanisms of RAF Kinases. *ChemBioChem, 20*(22), 2850-2861. https://doi.org/10.1002/cbic.201900266

Davies, H., Bignell, G. R., Cox, C., Stephens, P., Edkins, S., Clegg, S., et al. (2002). Mutations of the BRAF gene in human cancer. *Nature, 417*(6892), 949-954. https://doi.org/10.1038/nature00766

De Carlo, A., Ronchi, D., Piastra, M., Tosca, E. M., & Magni, P. (2024). Predicting ADMET properties from molecule SMILE: a bottom-up approach using attention-based graph neural networks. *Pharmaceutics, 16*(6), 776. https://doi.org/10.3390/pharmaceutics16060776

Favoni, R. E., & de Cupis, A. (1998). Steroidal and nonsteroidal oestrogen antagonists in breast cancer: basic and clinical appraisal. *Trends in pharmacological sciences, 19*(10), 406-415. https://doi.org/10.1016/s0165-6147(98)01252-8

Goh, T. B., Yian, K. R., Mordi, M. N., & Mansor, S. M. (2014). Antioxidant value and antiproliferative efficacy of mitragynine and a silane reduced analogue. Asian Pacific *Journal of Cancer Prevention, 15*(14), 5659-5665. https://doi.org/10.7314/APJCP.2014.15.14.5659

Harbeck, N., Penault-Llorca, F., Cortes, J., Gnant, M., Houssami, N., Poortmans, P., Ruddy, K., Tsang, J., & Cardoso, F. (2019). Breast cancer. *NatureRreviews Disease Primers, 5*(1), 66. https://doi.org/10.1038/s41572-019-0111-2

Hassan, S. S. U., Abbas, S. Q., Ali, F., Ishaq, M., Bano, I., Hassan, M., Jin, H., & Bungau, S. G. (2022). A Comprehensive *in silico* exploration of pharmacological properties, bioactivities, molecular docking, and anticancer potential of vieloplain F from *Xylopia vielana* Targeting B-Raf Kinase. *Molecules, 27*(3), 917. https://doi.org/10.3390/molecules27030917

Jornada, D. H., dos Santos Fernandes, G. F., Chiba, D. E., De Melo, T. R. F., Dos Santos, J. L., & Chung, M. C. (2015). The prodrug approach: a successful tool for improving drug solubility. *Molecules, 21*(1), 42. https://doi.org/10.3390/molecules21010042

Martinkovich, S., Shah, D., Planey, S. L., & Arnott, J. A. (2014). Selective estrogen receptor modulators: tissue specificity and clinical utility. *Clinical interventions in aging, 9*, 1437-1452. https://doi.org/10.2147/CIA.S66690

McGee, T. D., Edwards, J., & Roitberg, A. E. (2008). Preliminary molecular dynamic simulations of the estrogen receptor alpha ligand binding domain from antagonist to apo. *International Journal of Environmental Research and Public Health, 5*(2), 111-114. https://doi.org/10.3390/ijerph5020111

Priatna, P. A., Pratama, R. R., & Widyowati, R. (2023). Molecular docking estrogen receptor alpha antagonist and p53-mdm2 inhibitor, admet prediction of alkaloid compound from *Mitragyna speciosa* for breast cancer therapy. *Pharmacognosy Journal, 14*(6s), 912-916. https://doi.org/10.5530/pj.2022.14.188

Rahman, M. N. A., Nafiah, M. A., Wan, W. M. N. H., Salleh, S. P. T., Hashim, N. M., & Zamakshshari, N. H. (2022). Antioxidant, Antimicrobial, and Cytotoxic Activities of the Hexane and Dichloromethane extracts of Malaysian *Mitragyna spesioca* Korth. Leaves. *Malaysian Journal of Chemistry, 24*(2), 191-198

Salihu, A. S., Salleh, W. M. N. H. W., & Ogunwa, T. H. (2024). Computational exploration of flavonoids from the genus Knema with anti-inflammatory potential. *Journal of the Serbian Chemical Society, 89*(7-8), 1039-1051.https://doi.org/10.2298/JSC230904094S

Shanle, E. K., & Xu, W. (2010). Selectively targeting estrogen receptors for cancer treatment. *Advanced drug delivery reviews, 62*(13), 1265-1276. https://doi.org/10.1016/j.addr.2010.08.001

Shen, L., Pang, S., Zhong, M., Sun, Y., Qayum, A., Liu, Y., Rashid, A., Xu, B., Liang, Q., Ma, H., & Ren, X. (2023). A comprehensive review of ultrasonic assisted extraction (UAE) for bioactive components: Principles, advantages, equipment, and combined technologies. *Ultrasonics Sonochemistry, 101*, 106646.https://doi.org/10.1016/j.ultsonch.2023.106646

Shiau, A. K., Barstad, D., Loria, P. M., Cheng, L., Kushner, P. J., Agard, D. A., & Greene, G. L. (1998). The structural basis of estrogen receptor/coactivator recognition and the antagonism of this interaction by tamoxifen. *Cell, 95*(7), 927-937. https://doi.org/10.1016/s0092-8674(00)81717-1.

Smith, G. L., Lopez-Olivo, M. A., Advani, P. G., Ning, M. S., Geng, Y., Giordano, S. H., & Volk, R. J. (2019). Financial burdens of cancer treatment: a systematic review of risk factors and outcomes. *Journal of the National Comprehensive Cancer Network, 17*(10), 1184-1192. https://doi.org/10.6004/jnccn.2019.7305

Tian, Q., Wang, L., Sun, X., Zeng, F., Pan, Q., & Xue, M. (2019). Scopoletin exerts anticancer effects on human cervical cancer cell lines by triggering apoptosis, cell cycle arrest, inhibition of cell invasion and PI3K/AKT signalling pathway. *Journal of Balkan Union of Oncology, 24*(3), 997-1002. https://pubmed.ncbi.nlm.nih.gov/31424653/

Trott, O., & Olson, A. J. (2010). AutoDock Vina: improving the speed and accuracy of docking with a new scoring function, efficient optimization, and multithreading. *Journal of computational chemistry, 31*(2), 455-461. https://doi.org/10.1002/jcc.21334

Tsai, J., Lee, J. T., Wang, W., Zhang, J., Cho, H., Mamo, S., & Umar, A. B., Uzairu, A., Shallangwa, G. A., & Uba, S. (2020). QSAR modelling and molecular docking studies for anti-cancer compounds against melanoma cell line SK-MEL-2. *Heliyon, 6*(3). https://doi.org/10.1016/j.heliyon.2020.e03640

Wang, X., Zhang, H., & Chen, X. (2019). Drug resistance and combating drug resistance in cancer. *Cancer drug resistance, 2*(2), 141. https://doi.org/10.20517/cdr.2019.10

Zailan, N. F. Z., Zaidan, U. H., Mahayidin, H., & Hassan, M. (2019). *Mitragyna speciosa* methanol extract (MSME) exhibits potential anti-oxidative property and inhibitory activity on tumour growth stimulating cytokines in SW480 colorectal cancer cell lines. *Malaysian Journal of Medical Health Sciences, 15*(108), 35-35.